Soft Matter

RSC Publishing

HIGHLIGHT

Buckled colloidal monolayers connect geometric frustration in soft and hard matter

Cite this: *Soft Matter*, 2013, **9**, 6565

Yair Shokef,*[a] Yilong Han,[b] Anton Souslov,[c] A. G. Yodh[d] and Tom C. Lubensky[d]

Buckled monolayers of diameter-tunable microgel spheres constitute a soft-matter model system for studying geometric frustration in hard-condensed-matter antiferromagnetic materials. In the plane, the spheres self-assemble to form a triangular lattice. By considering the free volume available to two spheres slightly out of the plane, one finds an effective antiferromagnetic interaction; each pair of neighboring spheres prefers to be one up and one down. However, the topology of the triangular lattice prevents all pairs from simultaneously satisfying this rule. The micrometer length scale of the spheres enables direct visualization of the 'spin' dynamics at the single-particle level. These dynamics exhibit glassiness, which originates from the in-plane lattice distortions that partially relieve frustration and produce ground states with zigzagging stripes.

Received 8th January 2013
Accepted 20th February 2013

DOI: 10.1039/c3sm00069a

www.rsc.org/softmatter

I Geometric frustration

The close-packed triangular lattice constitutes the densest configuration of monodisperse disks on the plane. This packing maximizes density both globally and locally, *i.e.*, the most compact way to position neighboring disks around any given disk defines a hexagon that belongs to the globally preferred triangular lattice, see Fig. 1a. On the other hand, packing spheres in three-dimensional space is geometrically frustrating.[1] Locally, the optimal packing contains tetrahedral motifs of close-packed spheres.[2] However, tetrahedra do not fill space optimally,[3,4] and a perfect packing of tetrahedra cannot be extended to very large structures. Instead, the highest overall density is obtained by the face-centered cubic (fcc) lattice, which does not have local tetrahedral motifs and therefore maximizes

[a]*School of Mechanical Engineering, Tel-Aviv University, Tel-Aviv 69978, Israel. E-mail: shokef@tau.ac.il; Web: http://shokef.tau.ac.il*
[b]*Department of Physics, Hong Kong University of Science and Technology, Clear Water Bay, Hong Kong*
[c]*School of Physics, Georgia Institute of Technology, Atlanta, GA 30332, USA*
[d]*Department of Physics and Astronomy, University of Pennsylvania, Philadelphia, PA 19104, USA*

Yair Shokef completed his PhD in physics at the Technion – Israel Institute of Technology. During 2006–2008 he was a postdoctoral fellow at the University of Pennsylvania, where he focused on jamming and frustration in colloidal systems. During 2008–2011 he was a postdoctoral fellow at the Weizmann Institute of Science, where he deepened his interest in biophysics. Since 2011 he has been a faculty member at Tel-Aviv University. His research focuses on the non-equilibrium statistical mechanics of stuck and active soft-matter systems, ranging from frustration and jamming in colloidal systems and glasses to nonlinear elasticity and biologically driven fluctuations in living cells.

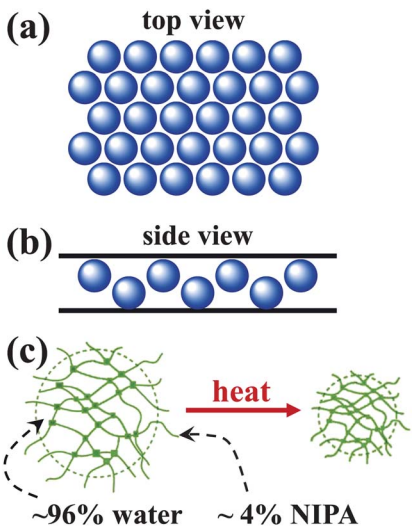

Fig. 1 Experimental setup. (a) The in-plane packing of a monolayer of spheres is a triangular lattice. (b) Out-of-plane, neighboring spheres have a tendency to move away from one another towards opposite walls. (c) Microgel spheres are composed of cross-linked NIPA polymers. When heated, the spheres shrink (deswell), and water is squeezed out such that the sample volume fraction is reduced, yet the spheres remain density-matched with the surrounding fluid.

density globally but not locally. Such frustration is responsible for the disorder and glassy dynamics[5] in a variety of concentrated soft-matter systems such as colloidal suspensions, emulsions, foams and granular matter.[6]

Interestingly, in many hard-condensed-matter systems ranging from ice[7] to antiferromagnets[8–10] and high-T_c superconductors,[11] a related inability to satisfy all local constraints due to geometric incompatibility also arises. The classic example of such geometric frustration is the antiferromagnetic Ising model,[12] the energy of which is minimized when each nearest-neighbor pair of spins adopts anti-parallel alignment. On a square lattice, this structure is easily achieved by the checkerboard arrangement of 'up' and 'down' spins shown in Fig. 2a. The triangular lattice, however, consists of three-particle plaquettes like the one highlighted in Fig. 2b, in which all neighboring spins cannot be mutually anti-parallel. In the ground state, the spins on two bonds of each triangular plaquette are anti-parallel and the spins on the third bond, which is frustrated, are parallel. Here the desired local order is that of two anti-parallel neighboring spins. When going to a slightly larger object of merely three particles, one cannot satisfy all the local two-particle rules. Although this famous model was the very first prototype of geometric frustration, it has rarely been achieved in real magnetic systems. In the last few years, however, significant progress has been made in fabricating "artificial" magnetic systems made of macroscopic building blocks that interact in a way that mimics the frustration found in the Ising model.[13–20]

In this paper, we highlight our recent efforts to study geometric frustration in soft matter, specifically in a novel, tunable colloidal model system consisting of a buckled monolayer of microgel spheres.[21] This soft-matter system, which mimics the triangular-lattice antiferromagnetic Ising model, enabled first studies of the single-particle dynamics originating from an analog of spin frustration in hard-condensed-matter systems. It thus serves as an important tool for advancing the understanding about frustration effects in both the soft- and hard-matter realms. We employed free-volume calculations to show how sphere-packing considerations can generate antiferromagnetic interactions in an effective Ising-model description of our colloidal system.[22] However, since the lattice is not rigid in our soft system, mapping to the Ising model on a triangular lattice is not exact. Positional degrees of freedom permit the colloidal monolayer to partially relieve geometric frustration through local deformations of the lattice,[21,22] which, in turn, are responsible for the structural and dynamical differences between our observations and the Ising-model predictions. Furthermore, frustration is often related to glassiness, and we have observed slow dynamics[21] and jamming,[22] which we can explain by mapping our experimental system onto an Ising model coupled to an elastic network of springs.[23] With this magneto-elastic interaction present, we exactly calculated[24] the minute differences in entropy between competing ground state configurations, which are a defining characteristic of various glassy systems.

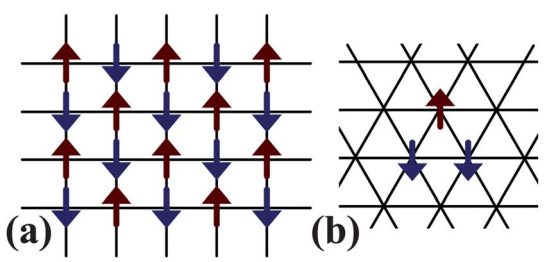

Fig. 2 Antiferromagnetic Ising model: (a) on the square lattice all spins can be mutually anti-parallel. (b) On the triangular lattice at least one pair of spins in each triangular plaquette must be parallel.

II Experiment

Buckled monolayers of colloidal spheres mimic the triangular-lattice antiferromagnetic Ising model.[25,26] We confined micrometer-sized colloidal spheres between parallel plates with about 1.5-sphere-diameter separation. At high enough densities the spheres self-assembled into a triangular lattice with buckled up or down states (Fig. 1) that are analogous to the up and down spin states of the Ising model. Using this analogy, we will refer to the up and down configurations of the colloidal particles as spin configurations. Neighboring spheres prefer opposite states (Fig. 1b) in order to have more free volume to move, *i.e.*, more entropy and less free energy. Thus they can be viewed as Ising spins with effective antiferromagnetic interactions. The analogy between buckled colloidal monolayers and Ising spins was first proposed in the early 1980's,[25,26] but at that time the experimentally observed crystalline domains were too small for meaningful measurements because wall spacing could not be made uniform enough. Most importantly, image processing techniques were not well developed, and therefore it was difficult to carry out quantitative measurements of these systems. In the work highlighted here, we generated large crystalline domains by using novel thermal-sensitive *N*-isopropyl acrylamide (NIPA) microgel spheres.[27] These spheres exhibit short-range repulsion,[28] and their hydrodynamic diameter decreases roughly linearly from 850 nm at $T = 20$ C to 650 nm at $T = 30$ C,[29] because NIPA polymers become less hydrophilic at higher temperatures (Fig. 1c). Thus, crucially, the ability to temperature-tune the particle diameter and sample packing fraction enabled us to vary the strength of the effective antiferromagnetic interaction between particles on the triangular lattice. Finally, since most of their volume is water, the spheres remain density-matched with the surrounding fluid, and gravitational effects are negligible.

Fig. 3a shows the monolayer at high temperature. The spheres self-assemble to form an in-plane triangular lattice. We focus our microscope image plane to a position in the top half of the experimental cell; in this case, spheres that are close to the top wall appear bright, whereas those close to the bottom wall are out of focus and appear darker. We measured a clear bimodal brightness distribution, indicating that spheres have a strong tendency to be close to either wall, rather than to stay in the center of the cell. Furthermore, we observed antiferromagnetic behavior, namely a statistical preference for neighboring spheres to be close to opposite walls.[21] As temperature is

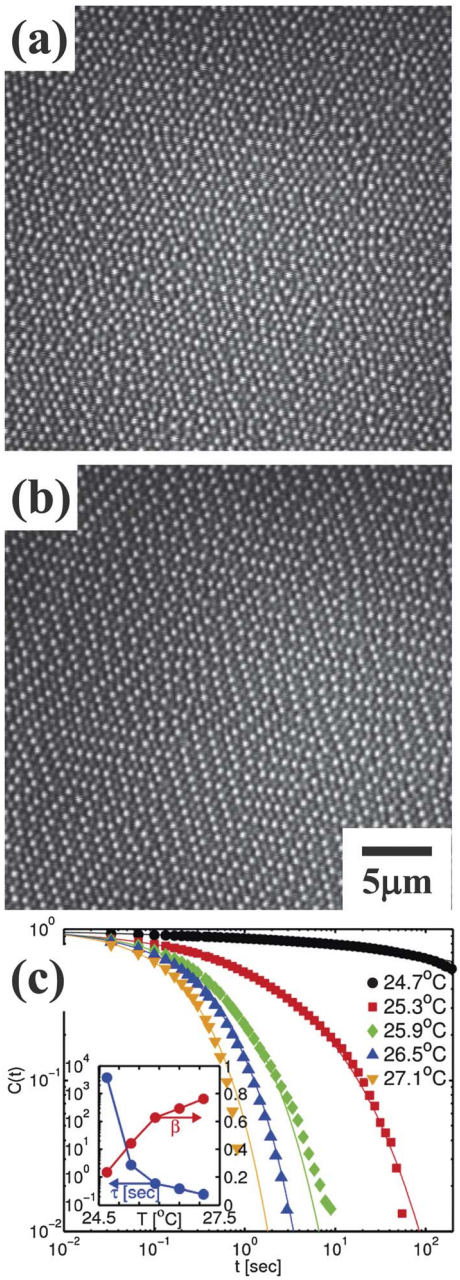

Fig. 3 Peculiar antiferromagnetic behavior. (a) At $T = 27.1$ C, the spheres form an in-plane triangular lattice, with roughly half of the spheres up (bright) and half down (dark), and with a statistical preference for neighboring spheres to be at opposite heights, as in an antiferromagnet. (b) At $T = 24.7$ C, the frustrated bonds form predominantly zigzagging stripes, which represent only a small fraction of the possible Ising model ground state. (c) The two-time correlation function $C(t) = \langle z_i(0)z_i(t)\rangle$ between the single-particle spin state, $z_i(t) = \pm 1$, decays as a stretched exponential of time, $C(t) = \exp[-(t/\tau)^{\beta}]$ with a relaxation time τ, which dramatically increases with decreasing temperature, and a stretching exponent β, which decreases toward zero as the temperature is decreased, see the inset. Figure adapted from ref. 21.

lowered, the sphere diameter increases, and the geometric, effective antiferromagnetic interaction between particles becomes stronger.[22] This effect leads to an increase in the measured probability of finding anti-parallel neighboring 'spins'. Despite this behavior, which generally agrees with the Ising model, we observed that at low temperature the frustrated bonds tend to arrange into parallel zigzagging stripes, as shown in Fig. 3b, instead of the more random distributions, which are preferred in the Ising model. We found that this discrepancy is due to the ability of the lattice to deform. This, in turn, can relieve some frustration and reduce the ground-state degeneracy from e^{N} in the Ising model to $e^{\sqrt{N}}$ here, *i.e.*, the zero-temperature entropy is reduced from extensive (S_0 N) to sub-extensive (S_0 $\sqrt{N}$), where N denotes the number of particles in the system.

Video microscopy of these micron-size colloidal particles enables us to identify the 'spin state' of each particle and also to track the Brownian dynamics of individual particles by image processing. Representative movies of the sample dynamics are available online in the ESI of ref. 21. As temperature is lowered these dynamics become slower; here we quantify the dynamics by the time autocorrelation function of the 'spin state' shown in Fig. 3c. These autocorrelation functions exhibit a stretched exponential decay, which can be viewed as a superposition of several exponential decays with different relaxation times. The overall relaxation time dramatically increases over a small temperature range.

III Isosceles tiling

We can understand why the observed zigzagging-stripe configurations are selected out of the multitude of disordered Ising ground-state configurations from the following packing arguments. At low temperature, the microgel spheres swell, and the system seeks configurations that enable close-packing of the colloidal spheres. For particles that are roughly hard spheres, the closest distance that two neighboring spheres can approach one another is equal to the sphere diameter d. For a frustrated bond (*i.e.*, two neighboring spheres close to the same wall), the vector connecting the sphere centers is in the plane of confinement. However, for a bond that satisfies the effective antiferromagnetic interaction (*i.e.*, neighbors wherein one

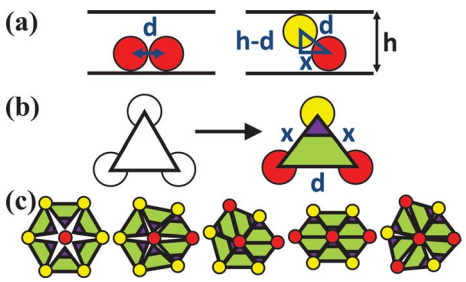

Fig. 4 Isosceles tiling: (a) the in-plane distance between a frustrated pair is the particle diameter d, while between a pair that manages to satisfy the effective antiferromagnetic interaction it is $x = \sqrt{d^2 - (h - d)^2} < d$. (b) For this reason, each triangular plaquette in the Ising ground state deforms to an isosceles triangle (in-plane) with two short edges x and one long edge d. (c) Of the configurations of a particle and its six neighbors that are allowed in the Ising ground state, the corresponding isosceles triangles tile the plane only when the central particle has exactly two frustrated neighbors. Up particles are colored yellow and down particles are red, and in each isosceles triangle, the head angle is marked in purple. Figure adapted from ref. 21.

sphere is close to the top wall, and one close to the bottom wall), this vector is tilted with respect to the horizontal direction, and its projection onto the plane of confinement gives a shorter in-plane distance, $x < d$, see Fig. 4a.

As a result, in the ground state of the antiferromagnetic Ising model, each triangular plaquette has one frustrated bond and will deform to an isosceles triangle with two bonds of length x and one bond of length d, see Fig. 4b. The close-packed state with the maximal density is then obtained by tiling the plane with such isosceles triangles. To see which spin states are compatible with this tiling requirement, we now consider possible configurations of a sphere and its six neighbors, which also defines six triangles around the central sphere, see Fig. 4c. We first require that each triangle contain only one frustrated bond. Up to rotations and spin inversions, the Ising-ground-state rule is satisfied in the five configurations shown in Fig. 4c. Of these five configurations, only two correspond to a fully space-filling tiling by isosceles triangular plaquettes. These two local states, selected by packing considerations, generate configurations of zigzagging stripes. Thus, each particle has two frustrated neighbors, and at each row the parallel stripes may continue on a straight line, or turn and bend, as shown experimentally in Fig. 1b and theoretically in Fig. 6b and c.

This structural difference between our colloidal antiferromagnet and the Ising model is also responsible for the different dynamical behavior we observe. In the Ising model, the ground state is not only disordered and highly degenerate, it also has high connectivity, *i.e.*, the system can evolve from one ground-state configuration to another by transitions that do not require any excitation energy and, thus, occur easily at arbitrarily low temperatures. This phenomenon is seen most clearly by the local zero-energy mode that the rightmost configuration in Fig. 4c represents. Here, the central particle has three frustrated bonds and three satisfied bonds, and thus has the same energy regardless of the spin state of the central particle. Flipping the central spin costs no energy and enables the system to more easily access all ground-state configurations.[30] It is also responsible for the rapid equilibration of the Ising model at any temperature. For our colloidal antiferromagnet, however, the local spin flip costs free-energy. Having no venue to relax, the system may get stuck in a metastable state, either relaxing very slowly,[21] or sometimes never reaching equilibrium.[22]

IV Order by disorder

Even though a frustrated system can have a highly degenerate ground state at zero temperature, at finite temperature entropy becomes relevant, and the free energy of hard-sphere-like systems is minimized by selecting the state with the greatest entropy. Thus, thermal fluctuations can induce order due to small fluctuations that are energetically softer than the excitations associated with the disordered ground-state configurations, see *e.g.*, ref. 9 and 31–36. Our tiling scheme proves that all possible realizations of zigzagging stripes have the same maximal density, which is the analog of the zero-temperature ground state. However, when the packing fraction is somewhat smaller than this maximal value (this corresponds to being at finite temperature), the thermodynamically stable state is the one with the largest free volume, and it is not clear which configuration has minimum free energy. This situation is similar to that which arises when packing spheres in three dimensions wherein the same maximal density may be obtained by stacking hexagonally packed layers, with any arbitrary sequence of lateral shifts, leading in the two limiting sequences to the fcc lattice and to hexagonal close packing (hcp). In this case, minute entropic differences are believed to select fcc over hcp,[37–46] but exact results are still lacking.

Before analyzing the entropic difference between straight and bent stripes, we consider the generic free-energy landscape of a glassy system. Typically, we expect to find in this landscape many local minima in which the system may be trapped and be metastable, plus a single (or slightly degenerate) minimum which is deeper than the others and is the equilibrium state of the system, see Fig. 5a. When rapidly cooled, the system often will get stuck in one of the metastable states; only if it is cooled extremely slowly, can the system reach the true equilibrium state. In our colloidal antiferromagnet, the free-energy landscape has a highly degenerate ground state, namely many minima (all at the same free energy), and what makes one configuration more stable thermodynamically than the others is the width, *i.e.*, the entropy associated with it, see Fig. 5b.

To calculate the free-volume contribution to the entropy of each zigzagging-stripe configuration, we approximate our colloidal system with an Ising model on an elastic network.[23,24] Namely, on top of the discrete, spin degrees of freedom, we now allow each spin to have a continuous displacement in the plane, see Fig. 5c. The total energy of the system is comprised of the antiferromagnetic interaction between neighboring pairs, the strength of which now decays linearly with the separation between them, together with an elastic energy representing the stretching or compression of the identical springs connecting

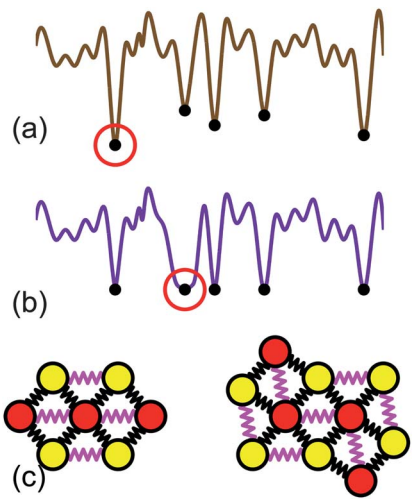

Fig. 5 Order by disorder: schematic representation of energy landscape in (a) glass, and (b) deformable Ising model. Red circles mark the lowest free-energy state, which the system prefers in equilibrium, *i.e.*, the lower energy state in (a), and the highest entropy state in (b). (c) Local configurations corresponding to straight and zigzag stripes in the elastic Ising model. Yellow and red circles represent up and down spins.

each pair of neighboring spins. Our treatment is related to previous work on magneto-elastic coupling in this context,[47,48] but it is more precise since we allow arbitrary deformations of the lattice.

For the deformable antiferromagnetic Ising model, the width of each free-energy minimum is related to the phonon spectrum around the corresponding deformed configuration, and we can thus exactly calculate the low-temperature entropic contribution of the phonons to the free energy. Interestingly, we found that for all values of the magneto-elastic coupling, straight stripes are entropically favored over zigzags.[24] This is consistent with theoretical arguments showing that generally the most anisotropic ground state configuration has the highest entropy.[33] We verified this result with numerical simulations in which our elastic Ising model was cooled at different rates. Fig. 6 shows that when rapidly cooled (panel a), only partial antiferromagnetic order is obtained, as can be seen from the fact that there are triangular plaquettes with all three particles in the same Ising state. For moderate cooling rate (panel b), the system reaches a configuration that belongs to the ground state of the Ising model (each plaquette contains only one frustrated pair), which has the aforementioned zigzagging-stripe structure. As the cooling rate is decreased even more (panel c), the persistence length of the stripes grows and they become closer to the straight stripes which constitute the equilibrium state we have predicted.

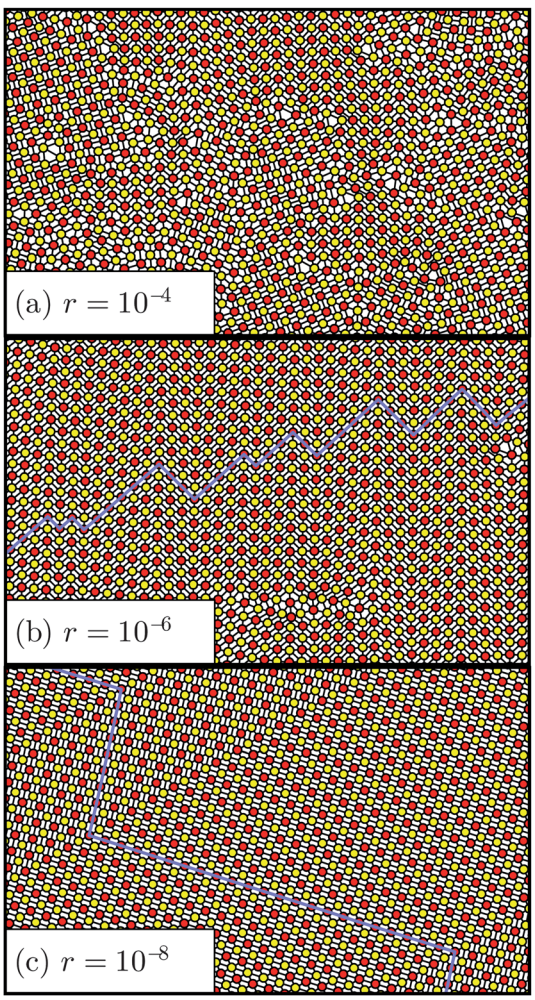

Fig. 6 Final configurations of our elastic Ising model for different cooling rates, r. Yellow and red circles represent up and down spins. Blue lines guide the eye to identify the zigzagging stripe patterns. Figure reproduced from ref. 24.

Although the equilibrium state is that of straight stripes, for virtually any preparation history the system gets jammed in a zigzagging stripe configuration. Such configurations are metastable only in a very weak sense, however, they have the same maximal packing fraction (corresponding to the energy in the Ising model) as straight-stripe configurations, and the only thermodynamic preference of straight stripes over zigzags is that straight stripes have a very small entropic advantage. However, passing between different close-packed states requires collective rearrangements involving the order of $\sqrt{N}$ particles, and requiring additional free-volume, which is not necessarily available for the system.

V Conclusions and outlook

In this paper, we have described our experimental and theoretical efforts to study a novel soft-matter system, consisting of diameter-tunable microgel spheres. When positioned between parallel plates that are separated by about 1.5 sphere diameters, the spheres self-assemble to form a buckled triangular-lattice monolayer. Packing considerations in the buckling of this monolayer generate effective interactions and frustration that are similar to those found in the antiferromagnetic Ising model on the triangular lattice. However, motion of the spheres in the plane of confinement partially relieves the frustration, giving rise to glassy dynamics and to partial order in the form of zigzagging stripes. Current techniques enable experimental tracking of the dynamics of individual particles in this soft-matter system, and thereby to learn about related frustration effects and frustration relaxation dynamics of hard-condensed matter magnetic materials. Moreover, we expect that the visualization of the single-particle dynamics in our colloidal system will directly advance the theoretical understanding of the dynamical properties of various currently studied mesoscopic frustrated systems.[13–20]

Future work on our colloidal antiferromagnet should focus on analyzing its non-equilibrium dynamics. For example, by manipulating individual particles with laser tweezers, one could measure spatio-temporal correlations between different particles in the system, and use this information to learn about relaxation processes in glassy materials. Furthermore, with holographic optical tweezers,[49–51] one could bring the system to an arbitrary configuration, and monitor the relaxation processes that will occur after the trapping potential is turned off. Finally, it would be interesting to relate the packing frustration investigated here to that found in other colloidal systems such as self-assembled Janus particles,[52,53] colloidal spheres packed in narrow tubes,[54–57] and to the aforementioned fcc *vs.* hcp question.[40]

Acknowledgements

We thank Ahmed Alsayed, Chris Henley, Valery Ilyin, Randy Kamien, Andrea Liu, Itamar Procaccia, Ido Regev, and Peter Yunker for helpful discussions and technical assistance. This

work was supported by National Science Foundation grants DMR12-05463, PENN-MRSEC-DMR11-20901, by NASA grant NNX08AO0G, and by Israel Science Foundation grants 617/12, 1730/12.

References

1 J.-F. Sadoc and R. Mosseri, *Geometrical frustration*, Cambridge University Press, Cambridge, UK, 1999.
2 A. B. Hopkins, F. H. Stillinger and S. Torquato, *Phys. Rev. E: Stat., Nonlinear, Soft Matter Phys.*, 2011, **83**, 011304.
3 E. R. Chen, M. Engel and S. C. Glotzer, *Discrete Comput. Geom.*, 2010, **44**, 253.
4 S. Gravel, V. Elser and Y. Kallus, *Discrete Comput. Geom.*, 2011, **46**, 799.
5 G. Tarjus, S. A. Kivelson, Z. Nussinov and P. Viot, *J. Phys.: Condens. Matter*, 2005, **17**, R1143.
6 A. J. Liu and S. R. Nagel, *Annu. Rev. Condens. Matter Phys.*, 2010, **1**, 347.
7 L. Pauling, *J. Am. Chem. Soc.*, 1935, **57**, 2680.
8 S. T. Bramwell and M. J. P. Gingras, *Science*, 2001, **294**, 1495.
9 R. Moessner, *Can. J. Phys.*, 2001, **79**, 1283.
10 S. Nakatsuji, Y. Nambu, H. Tonomura, O. Sakai, S. Jonas, C. Broholm, H. Tsunetsugu, Y. Qiu and Y. Maeno, *Science*, 2005, **309**, 1697.
11 P. W. Anderson, *Science*, 1987, **235**, 1196.
12 G. H. Wannier, *Phys. Rev.*, 1950, **79**, 357.
13 H. Hilgenkamp, Ariando, H. J. H. Smilde, D. H. A. Blank, G. Rijnders, H. Rogalla, J. R. Kirtley and C. C. Tsuei, *Nature*, 2003, **422**, 50.
14 J. R. Kirtley, C. C. Tsuei, Ariando, H. J. H. Smilde and H. Hilgenkamp, *Phys. Rev. B*, 2005, **72**, 214521.
15 G. Moller and R. Moessner, *Phys. Rev. Lett.*, 2006, **96**, 237202.
16 R. F. Wang, C. Nisoli, R. S. Freitas, J. Li, W. McConville, B. J. Cooley, M. S. Lund, N. Samarth, C. Leighton, V. H. Crespi and P. Schiffer, *Nature*, 2006, **439**, 303.
17 A. Libal, C. Reichhardt and C. J. Olson Reichhardt, *Phys. Rev. Lett.*, 2006, **97**, 228302.
18 C. Nisoli, R. Wang, J. Li, W. F. McConville, P. E. Lammert, P. Schiffer and V. H. Crespi, *Phys. Rev. Lett.*, 2007, **98**, 217203.
19 P. E. Lammert, X. Ke, J. Li, C. Nisoli, D. M. Garand, V. H. Crespi and P. Schiffer, *Nat. Phys.*, 2010, **6**, 786.
20 P. Mellado, A. Concha and L. Mahadevan, *Phys. Rev. Lett.*, 2012, **109**, 257203.
21 Y. Han, Y. Shokef, A. M. Alsayed, P. Yunker, T. C. Lubensky and A. G. Yodh, *Nature*, 2008, **456**, 898.
22 Y. Shokef and T. C. Lubensky, *Phys. Rev. Lett.*, 2009, **102**, 048303.
23 V. Ilyin, I. Procaccia, I. Regev and Y. Shokef, *Phys. Rev. B*, 2009, **80**, 174201.
24 Y. Shokef, A. Souslov and T. C. Lubensky, *Proc. Natl. Acad. Sci. U. S. A.*, 2011, **108**, 11804.
25 P. Pieranski, L. Strzelecki and B. Pansu, *Phys. Rev. Lett.*, 1983, **50**, 900.
26 T. Ogawa, *J. Phys. Soc. Jpn.*, 1983, **52**, 167.
27 R. Pelton, *Adv. Colloid Interface Sci.*, 2000, **85**, 1.
28 Y. Han, N. Y. Ha, A. M. Alsayed and A. G. Yodh, *Phys. Rev. E*, 2008, **77**, 041406.
29 A. M. Alsayed, M. F. Islam, J. Zhang, P. J. Collings and A. G. Yodh, *Science*, 2005, **309**, 1207.
30 Y. Han, *Phys. Rev. E*, 2009, **80**, 051102.
31 J. Villain, R. Bidaux, J. P. Carton and R. Conte, *J. Phys.*, 1980, **41**, 1263.
32 C. L. Henley, *J. Appl. Phys.*, 1987, **61**, 3962.
33 C. L. Henley, *Phys. Rev. Lett.*, 1989, **62**, 2056.
34 A. Chubukov, *Phys. Rev. Lett.*, 1992, **69**, 832.
35 J. N. Reimers and A. J. Berlinsky, *Phys. Rev. B*, 1993, **48**, 9539.
36 D. Bergman, J. Alicea, E. Gull, S. Trebst and L. Balents, *Nat. Phys.*, 2007, **3**, 487.
37 F. H. Stillinger and Z. W. Salsburg, *J. Chem. Phys.*, 1967, **46**, 3962.
38 B. J. Alder, W. G. Hoover and D. A. Young, *J. Chem. Phys.*, 1968, **49**, 3688.
39 W. G. Rudd, Z. W. Salsburg, A. P. Yu and F. H. Stillinger, *J. Chem. Phys.*, 1968, **49**, 4857.
40 P. N. Pusey, W. van Megen, P. Bartlett, B. J. Ackerson, J. G. Rarity and S. M. Underwood, *Phys. Rev. Lett.*, 1989, **63**, 2753.
41 L. V. Woodcock, *Nature*, 1997, **385**, 141.
42 P. G. Bolhuis, D. Frenkel, S. C. Mau and D. A. Huse, *Nature*, 1997, **388**, 235.
43 L. V. Woodcock, *Nature*, 1997, **388**, 236.
44 S. C. Mau and D. A. Huse, *Phys. Rev. E*, 1999, **59**, 4396.
45 C. Radin and L. Sadun, *Phys. Rev. Lett.*, 2005, **94**, 015502.
46 H. Koch, C. Radin and L. Sadun, *Phys. Rev. E*, 2005, **72**, 016708.
47 Z. Y. Chen and M. Kardar, *J. Phys. C: Solid State Phys.*, 1986, **19**, 6825.
48 L. Gu, B. Chakraborty, P. L. Garrido, M. Phani and J. L. Lebowitz, *Phys. Rev. B*, 1996, **53**, 11985.
49 E. R. Dufresne and D. G. Grier, *Rev. Sci. Instrum.*, 1998, **69**, 1974.
50 J. E. Curtis, B. A. Koss and D. G. Grier, *Opt. Commun.*, 2002, **207**, 169.
51 D. G. Grier, *Nature*, 2003, **424**, 810.
52 S. Granick, S. Jiang and Q. Chen, *Phys. Today*, 2009, **62**, 68.
53 Q. Chen, S. C. Bae and S. Granick, *Nature*, 2011, **469**, 381.
54 J. H. Moon, S. Kim, G. R. Yi, Y. H. Lee and S. M. Yang, *Langmuir*, 2004, **20**, 2033.
55 F. Li, X. Badel, J. Linnros and J. B. Wiley, *J. Am. Chem. Soc.*, 2005, **127**, 3268.
56 M. Tymczenko, L. F. Marsal, T. Trifonov, I. Rodriguez, F. Ramiro-Manzano, J. Pallares, A. Rodriguez, R. Alcubilla and F. Meseguer, *Adv. Mater.*, 2008, **20**, 2315.
57 M. A. Lohr, A. M. Alsayed, B. G. Chen, Z. Zhang, R. D. Kamien and A. G. Yodh, *Phys. Rev. E*, 2010, **81**, 040401.

